CONF-831203--69

CONF-831203--69

DE84 004568

END CELL I&C REQUIREMENTS FOR OPERATING TANDEM MIRROR REACTORS*

G. E. Gorker
Fusion Engineering Design Center
Oak Ridge National Laboratory
P.O. Box Y
Oak Ridge, Tennessee 37831

John E. Osher
Lawrence Livermore National Laboratory
University of California
P.O. Box 808
Livermore, California 94550

Abstract: The next generation of fusion reactors will be developed to achieve near-ignition conditions and operate in a tritium environment for significant periods of time. Radiation-hardened diagnostic instrumentation must be developed for these reactors. Although neutral beam injection (NBI) will be used for plasma heating and fueling of experimental fusion machines like MFTF-α+T, it is believed that ion cyclotron resonance heating (ICRH) will be used in future machines for heating the plasma. When rf heating is used, fueling will be accomplished with gas puffing and advanced fuel injectors. End cell coils, NBI, and microwave power injectors are needed to provide adequate confinement. Microwave power and NBI control the electrostatic potentials of the plug and barrier. Low-frequency rf power provides drift pump control of the ions so that they are lost radially, enhancing the use of direct converters that collect the axially flowing electrons. Direct or indirect measurements of electrostatic potential barriers, electron density, and temperature appear necessary to control the NBI and microwave power generators. This paper discusses some of the end cell instrumentation and control (I&C) systems believed to be necessary for tandem mirror reactors.

Introduction

The I&C requirements discussed in this paper are for a small experimental tandem mirror reactor, a proposed upgrade of the Mirror Fusion Test Facility (MFTF-B) known as MFTF-α+T (see Ref. 1). The upgrade consists of adding a central cell insert and modifying the end cells so that reactor components can be tested in a fusion environment for 1 to 100 h. The α+T end cell has the same configuration as the proposed Mirror Advanced Reactor Study (MARS) tandem mirror reactor for generating commercial electricity. The central cell, with its insert, is different from the MARS design. Therefore, most of this paper is devoted to the I&C for the end cells, each of which consists of an anchor cell, a plug cell, and a direct converter.

Figure 1 shows the MFTF-α+T magnet configuration and the desired field on axis. Normally, a tandem mirror reactor will not have the small inside axicell mirror for testing materials and components. Figure 2 is a three-dimensional view that identifies the regions of the end cell group: the zone of the first Yin-Yang pair following the transition coil is defined as the anchor cell; the zone of the second Yin-Yang pair is defined as the plug cell. A transition coil and recirculating coil beyond the plug cell are needed to accommodate the circular direct converter (not shown in the figure).

Operating Modes and Their Requirements

The MFTF-α+T has two modes of operation: a high-Q mode and a high-Γ mode. In the high-Q mode, the thermal power amplification Q = 2.4; in the high-Γ mode, the wall loading of the central axicell Γ = 2.0 MW/m^2. Figures 3 and 4 show the required axial profiles of the magnetic field, plasma density, and plasma potential, as well as some of the rf and NBI used to achieve the plasma profiles. For this paper, the axicell plasma is maintained at ground potential and other potentials are made relative to ground. Note that the direct converter potential is -79 kV for the high-Q mode but only -47 kV for the high-Γ mode. The corresponding potential barrier peaks in the plug cells are 62 kV and 22 kV, respectively. Therefore, the end cell controls must cover a fairly wide range to accommodate both control modes.

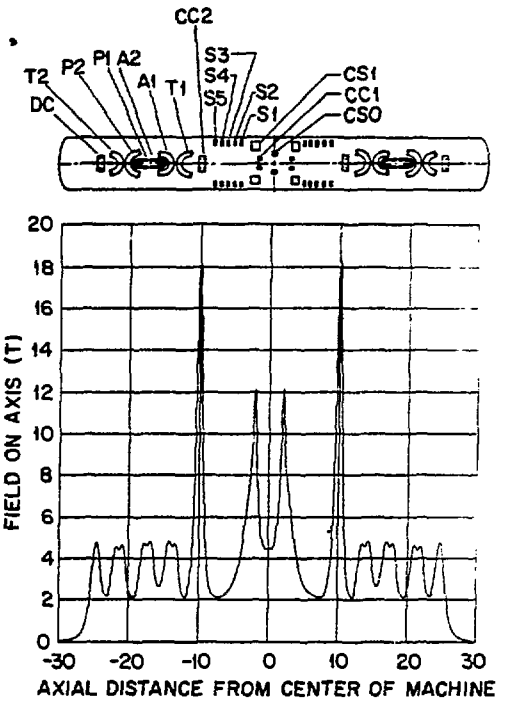

Fig. 1. MFTF-α+T magnet identification and field on axis.

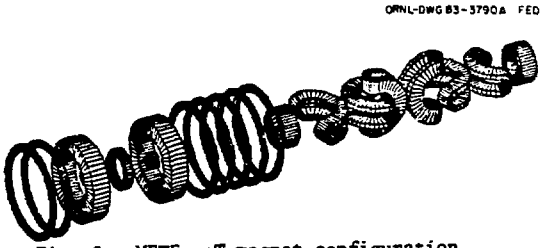

Fig. 2. MFTF-α+T magnet configuration.

*Research sponsored by the Office of Fusion Energy, U.S. Department of Energy, under Contract No. W-7405-eng-26 with the Union Carbide Corporation.

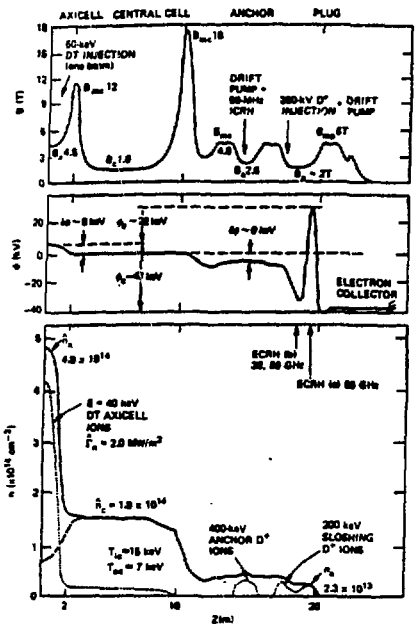

Fig. 3. Profiles of field, potential, and density in the high-Q mode.

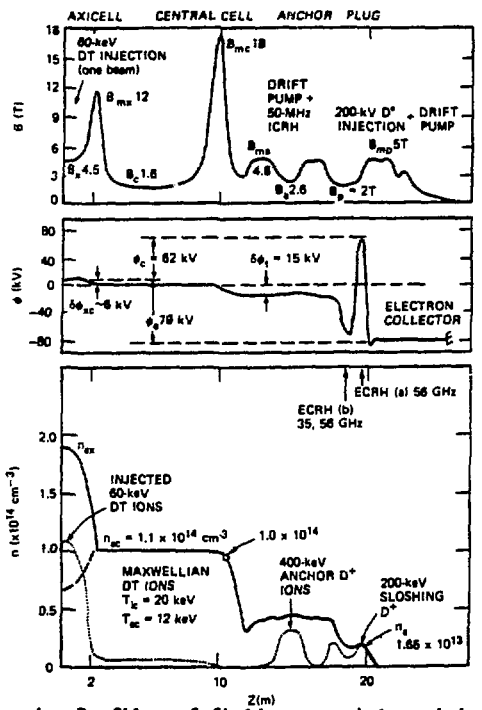

Fig. 4. Profiles of field, potential, and density in the high-Γ mode.

Basis for the I&C Requirements

Several alternatives could be pursued that vary between the minimum I&C to operate the machines and the ultimate that may be needed to develop and prove controls for the Fusion Demonstration Plant (FPD) and MARS. Previous work [2] emphasizes the need for real-time, radiation-hardened plasma diagnostics that will operate reliably in a fusion environment. Providing the additional programmable controls will cost far less than the off-line diagnostics needed for the minimum system. Therefore, MFTF-α+T should also be designed for developing and testing diagnostics that can be used for control future tandem mirror reactors.

Architecture of the Control Systems

Seven major zones require I&C to create and maintain the typical profiles given in Figs. 3 and 4. Table 1 identifies these zones, the equipment being controlled, the measured controlling process variables, and the diagnostic measure or variable of direct interest that might be considered for trim correction control. Although the variables identified in the third column are the ones of greatest interst, they are also the most difficult to measure reliably on a real-time basis. Magnetic field on axis can be measured and correlated with magnet currents long before the machine becomes operational. There is no real need to make these measurements thereafter. (The actual alignment of the large magnets is difficult and requires the use of alignment coils to obtain the desired magnetic field.)

Table 1. Tandem mirror control measurements

Control	Process Measure	Diagnostic Measure
Axicell and Central Cell		
D2 and T2 fueling NBI power supply voltages	D2 and T2 NBI currents	• Plasma ion temperature • Plasma density • Neutron flux (maximize)
D2 gas injector flow	Background gas pressure	Warm plasma density
SC magnet power supply voltages	SC magnet currents	Magnetic field
RC magnet power supply voltages	RC magnet currents	Magnetic field
East and West Transition and Anchor Cells		
Drift pump rf power gain	Low frequency rf power	Electromagnetic fluctuations (minimize)
ICRH power supply voltages	ICRH power	• Ion energy • Ion density
SC magnet power supply voltages	SC magnet currents	Magnetic field
D2 gas injector flow	Background gas pressure	Warm plasma density
East and West Plug Cells and Transition		
Negative NBI power supply voltages	Deuterium NBI currents	Ratio of plasma density at point (a) to plasma density at point (b)
600-kHz drift pump power gain	RF power	Plasma density at point (b) relative to point (a)
56-GHz ECRH power supply voltages	ECRH power	Plasma potential and electron density at point (a)
35/56-GHz power supply voltages	ECRH power	Ratio of plasma potential point (a) to point (b)
SC magnet power supply voltages	SC magnet currents	Magnetic field
East and West Direct Converters		
Direct converter load resistance	Collector voltages	Collector currents (Collector power)

Figure 5 is a general block diagram showing the measured process variables, the diagnostic variables, and their relationship to the equipment being controlled. Table 2 defines the mnemonics used in this paper. The lower part of the figure identifies the I&C for operating the plasma-confining magnets, and the upper part identifies the I&C for controlling plasma heating and fueling, plug cell potential, and the direct conversion voltage. Only one of the two end cell regions is shown in the figure.

In the upper part of Fig. 5, the process variables that can be measured reliably are compared to their scheduled demands, which are integrated with the use

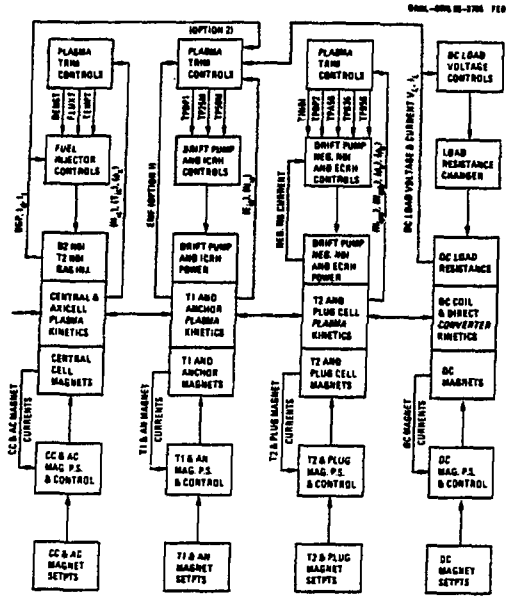

Fig. 5. Overall α+T control system diagram.

Table 2. Mnemonic Definitions

ACCEL	Acceleration
BGP	Background gas pressure, torr
CC	Central cell
D2	Deuterium isotope of hydrogen
Eia	Energy of anchor cell ions
EMF	Electromagnetic fluctuations
HI Γ	High wall heat loading mode of operation
HI Q	High power amplification mode of operation
Id	Total deuterium NBI current, amperes
It	Total tritium NBI current, amperes
Nia	Ion density in the anchor cell
Nipa	Ion density at point (a) of the plug cell
Nipb	Ion density at point (b) of the plug cell
NBI	Multiple source neutral beam injector
NBSX	Negative NBI source power supply number X
P.S.	Power supply
RC	Resistive conductor
SC	Superconductor
SETPTS	Controller setpoint inputs
TINBI	Trim control input to the negative NBI of the plug cells
TPA56	Trim input to 56-GHz ECRH power control of point (a) of the plug cell
TPB35	Trim input to 35-GHz ECRH power control of point (b) of the plug cell
TPB56	Trim input to 56-GHz ECRH power control of point (b) of the plug cell
TP25M	Trim input to 25-MHz ICRH power control of the anchor cell
TP50M	Trim input to 50-MHz ICRH power control of the anchor cell
TPDP1	Trim input to the drift pump rf power control of the plug cell
<Y>	Line average of variable Y across the plasma
φa	Electrostatic potential at point (a) of plug cell
φb	Electrostatic potential at point (b) of plug cell

of a synchronous timer (shown in more detail for one of the control systems in Fig. 6). A function of the error signal controls the NBI currents; the ICRH, electron cyclotron resonance heating (ECRH), and drift pump rf power; the direct converter voltage; and the gas injection flow. These programmable process controllers continually operate without any input from the secondary plasma trim controllers, shown in the upper part of Fig. 5. As reliable real-time diagnostics are developed and hardened, they can be used to correct the primary controllers to optimize the generation of the profiles shown in Figs. 3 and 4. Until suitably hardened on-line diagnostics become available, the programmable demand schedules are adjusted by trial and error to optimize the performance using off-line measurements of the diagnostic variables.

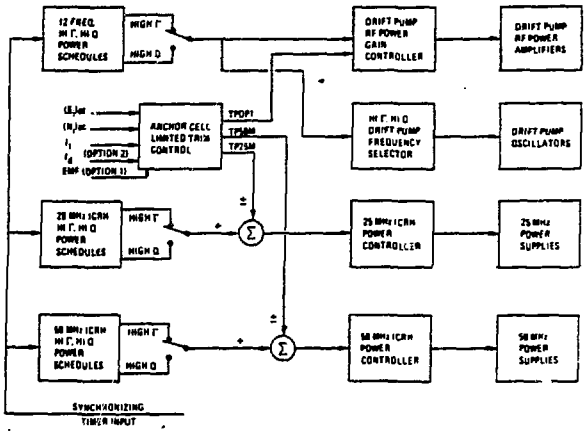

Fig. 6. Anchor cell control system.

There are many MFTF-α+T control systems that are not considered here. The MFTF-B magnet control and protection systems applicable to this upgrade have been described in Refs. 3 and 4. Only the anchor cell and plug cell I&C are addressed in more detail here.

Anchor Cell ICRH and Drift Pump Control

The function of the ICRH and the rf drift pumps in the anchor cell is to selectively remove the unwanted ions by radial pumping so that they are collected and removed at the halo scraper. The electrons are removed axially and collected at the direct converter. To perform this function, the anchor cell employs 12 rf drift pump frequencies ranging from 56 kHz to 96 kHz and two ICRH systems. One ICRH system injects 25-MHz power and the other injects 50-MHz power for heating ions to about 400 keV. In the high-Q mode, the drift pump antenna power is about 65 kW, and the ICRH antenna power is about 700 kW at 25 MHz and 130 kW at 50 MHz. In the high-Γ mode, the drift pump antenna power is about 230 kW and the ICRH antenna power is about 800 kW at 25 MHz and 340 kW at 50 MHz. The following requirements are based on a 1-s start-up of the end cell:

- Control system response time will be about 0.1 s.
- Drift pump and ICRH power will have programmable controls for operating between 10% and 100% of the maximum design point power of the high-Γ mode.
- Absolute accuracy will be equal to or better than ±5% of the demand setpoint. Regulation will be ±1% or better.

- Loss of cooling to water-cooled components will turn off the ICRH and rf drift pump power supplies within 0.1 s.

Figure 6 is a block diagram of the control system for one anchor cell. The operating mode is selected by the operator. The synchronizing timer provides a timing signal to the demand schedules that generate the demand input to the controllers. The drift pump gain is set to deliver the required antenna power for each of the 12 frequencies in the high-Q mode and 10 frequencies in the high-Γ mode. The demand schedule selects the required frequencies. Likewise, the ICRH power demand is generated as input to the ICRH function table controller, which selects the power supply voltages corresponding to the desired power. All these controllers can be initially open-ended; that is, the actual rf power is not measured and used as a feedback control signal. Later, as real-time diagnostic instrumentation is developed and proven, feedback trim correction can be applied to optimize the performance.

The requirements for the feedback diagnostic trim controller are given in Ref. 5. A more detailed diagram of some control options is given in Fig. 7. The ICRH power is controlled by measuring the hot ion energy and density, which are converted to a power correction signal. Until the diagnostic is proven, the proportional gain control is set to zero. A ratio control is provided to split the correction between the ICRH power injectors.

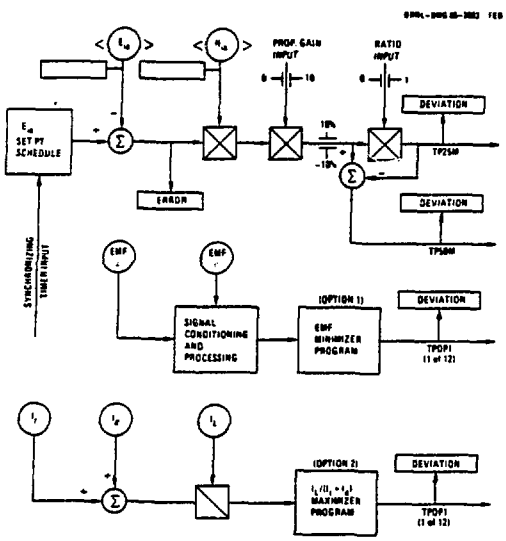

Fig. 7. Anchor cell plasma trim control system.

There are many small rf drift pump generators operating at different frequencies. During initial operations, their powers will be equal. Two control options are shown in Fig. 7. Option 1 controls the deviation correction to minimize the electromagnetic fluctuation measurements. Option 2 measures the direct converter load current and the NBI currents to the central cell and controls the deviation to maximize the available current to the direct converter. The optimizer programs can adjust the distribution of deviations, which initially are all set to zero.

Plug Cell ECRH, NBI, and Drift Pump Control

The function of the ECRH, the sloshing-ion neutral beam injector, and the rf drift pump of the plug cells is to establish and maintain the maximum potential at point (a) and the minimum potential at point (b) of Figs. 3 and 4. These potentials establish confinement barriers for both ions and electrons and assist the anchor cell components in radially pumping the ions. To perform these functions, the plug cell uses a negative 10-A beam injector, three ECRH injector systems, and a frequency-modulated (FM) drift pump that sweeps between 560 kHz and 640 kHz every 0.1 s. The three ECRH systems supply rf energy to heat the plug cell electrons at points (a) and (b). The ECRH frequencies, injected power, and injection location for the high-Q and high-Γ modes are given in Table 3. The table also lists similar data for the FM drift pump, whose energy is not concentrated at a point, and for the neutral beam injection, whose energy is concentrated at the image of point (a). The following requirements are based on a 1-s start-up of the end cells:

- Response time of the control systems will be about 0.1 s.
- Drift pump and ECRH power will have programmable controls for operating between 10% and 100% of the maximum design point power.
- Neutral beam injectors will have programmable current and acceleration voltage controls for operating between 40% and 100% of the design currents and voltages.
- Absolute accuracy of the rf power inputs will be ±5% of the demand setpoint. Regulation will be ±1% or better.
- NBI currents will have a regulation of ±1% of the design point current.
- Loss of cooling to the NBI or rf power equipment will turn off their power supplies within 0.1 s.
- NBI sources will be able to automatically restart when high-voltage breakdown or arc quench occurs so that long-term operation is not interrupted.

Table 3. Plug cell power injection for the high-Q and high-Γ modes

System	Incident power (kW) High Q	Incident power (kW) High Γ	Frequency (GHz)	Location (Point)
ECRH-1	384	600	35	(b)
ECRH-2	360	480	56	(b)
ECRH-3	72	120	56	(a)
FM drift pump	65	24	600 KHz	N.A.
200-keV NBI	840	440	N.A.	(a')

Figures 8 and 9 are block diagrams of the proposed control system for one plug cell. The control mode is selected by the operator. The synchronous timer drives the demand schedule function generators. The NBI current and voltage controllers set the voltages of the programmable power supplies. The operation of the ECRH control systems is like that described for the ICRH of the anchor cells, where the power is indirectly controlled by setting the voltages of the power supplies. The power of the FM drift pump is indirectly controlled with programmable gain controls.

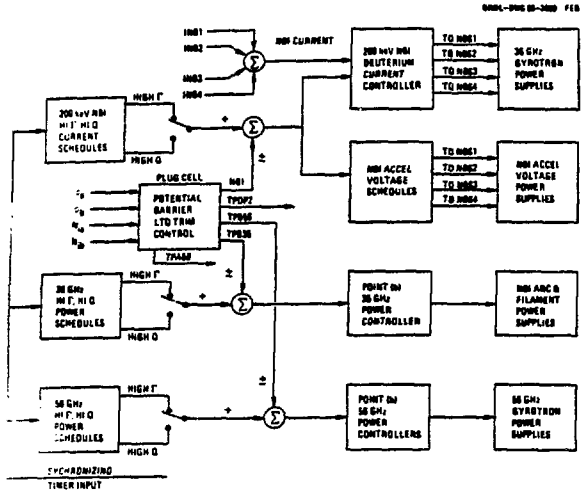

Fig. 8. Block diagram of MFTF-α+T plug cell potential control system.

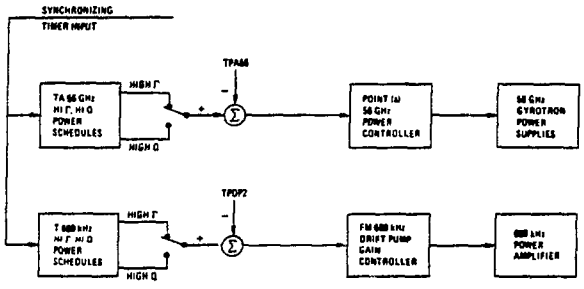

Fig. 9. Plug cell potential control system.

The proposed plug cell trim correcting feedback controllers are shown in Fig. 10. Their requirements are given in Ref. 5. The trim controls are intended to measure the plasma density and potential at points (a) and (b). Proportional gain controls are initially set to zero until the diagnostic measurements are calibrated and proven. Proportional gain controls are then increased to provide feedback correction. A ratio control is provided to split the power correction between the 35-GHz and 56-GHz ECRH systems that inject power at point (b).

Conclusions

The physics model of the tandem mirror end cells is under continuing development. Experiments will be required during the DD operating phase to provide guidelines for establishing the optimum relationships between variables. Primary controls must be programmable so that the scheduled parameters and optimizing strategies can be varied to accommodate changes in DT operation and alpha heating. The machine should be designed for developing hardened diagnostics that provide real-time measurements of plasma density, plasma temperature, and other parameters defined in Table 4. Front-surface mirrors need to be hardened for long exposure to direct plasma radiation from the axicell and central cell for optical diagnostic measurements of plasma density, temperature, and impurities in these cells. Installing real-time diagnostic controllers on a timely basis will accelerate their use on MFTF-α+T and future reactors.

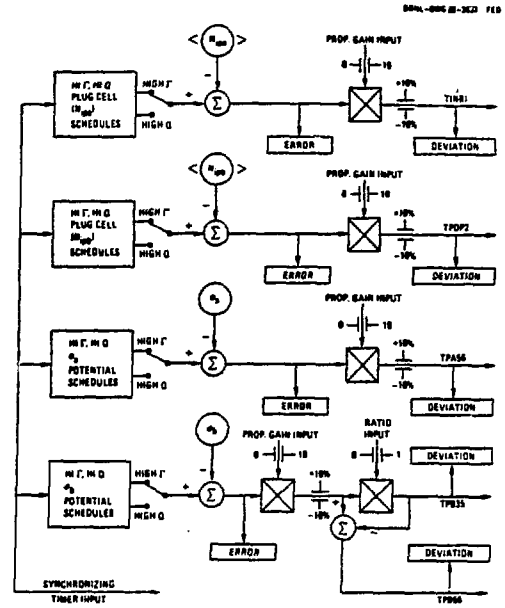

Fig. 10. Plug cell plasma trim control system.

Table 4. Required hardened end cell diagnostics

Number	Diagnostic	Measured parameter
5	Ion spectrometers (ISP)	Radial profile of maximum plug potential
10	Charged particle flux (CPF)	Radial profile of axial charged particle flux
10	Calorimeters (CAL)	Radial profile of axial radiant power
5	Hard x-ray emission from an aluminum or steel target plate	Radial profile of mean electron temperature or energy in the hot plug and barrier regions
5	Sensitive high-energy neutron flux detectors	Radial profile of high-energy, axially directed neutrons

References

[1] J. N. Doggett and K. I. Thomassen, "Options to Upgrade the Mirror Fusion Test Facility," UCID-19743, Lawrence Livermore National Laboratory, April 1983.

[2] J. F. Baur et al., "Radiation Hardening of Diagnostics for Fusion Reactors," GA-A16614, General Atomic Company, December 1981.

[3] S. T. Wang et al., "The Axicell MFTF-B Superconducting Magnet System," in Proceedings of the 9th International Cyrogenic Engineering Conference, 1983, pp. 424-433.

[4] T. A. Kozman et al., "Magnets for the Mirror Fusion Test Facility," IEEE Trans. Magn., Vol. MAG-19, No. 3, pp.859-866, May 1983.

[5] W. D. Nelson, J. N. Doggett, and J. A. O'Toole, "MFTF-α+T Progress Report," ORNL/FEDC-83/9, Oak Ridge National Laboratory, to be published.

DISCLAIMER